Solar Physics (2005) 228: 29–42

MULTIFRACTAL ANALYSIS OF SOLAR MAGNETOGRAMS

VALENTYNA I. ABRAMENKO
Big Bear Solar Observatory, 40386 N. Shore Lane, Big Bear City, CA 92314, U.S.A.;
Crimean Astrophysical Observatory, 98409 Nauchny, Crimea, Ukraine
(e-mail: avi@bbso.njit.edu)

(Received 31 January 2005; accepted 24 February 2005)

Abstract. As solar observational techniques improve, fine small-scale structures observed on the solar surface become more pronounced. Complex filigree structures of solar granulation, sunspots, photospheric magnetic and velocity fields cannot be described adequately by a single parameter (e.g., filling factor, fractal dimension, or power-law index). Methods which incorporate parameters that are a function of scale (multiscale methods) to describe the complexity of a field under study, should be involved. The multifractal approach offers such a possibility. In this paper the scaling of structure functions is proposed in order to analyze multifractality. Application of the approach to SOHO/ MDI high-resolution magnetograms of active regions show that the structure functions differ for all active regions studied. For a given active region, the functions may maintain their shape during several hours; however, they can significantly change during a day. Flare-quiet active regions tend to possess a lower degree of multifractality than flaring active regions do. The increase in multifractality is a signal that a magnetic structure is driven to a critical state, thus gaining tangential discontinuities of various length scales.

1. Introduction

Luxuriant and filigree character of structures observed on the Sun impels us to apply fractal methods (Mandelbrot, 1977; Feder, 1988; Takayasu, 1989) in order to learn more about these structures, in particular, about magnetic fields (Balke *et al.*, 1993; Meunier, 1999; Lawrence, Ruzmaikin, and Cadavid, 1993; McAteer, Gallagher, and Ireland, in press).

A fractal is an object whose parts somehow resemble the whole, or, to put it in more rigorous way, a self-similar, scale-invariant structure without any characteristic length (Feder, 1988; Takayasu, 1989).

In this paper I concentrate on two-dimensional fractals. Several approaches were elaborated to explore the fractal nature of 2D geometrical objects. The approaches differ by mathematical measures introduced on the geometrical object (Takayasu, 1989; Lawrence, Ruzmaikin, and Cadavid, 1993). The method proposed in the present paper (Section 2) is based on a measure defined by structure functions. However, in order to illustrate the idea of multifractality in the Introduction, I will use the most popular approach based on a probability measure, which leads to a notion of a fractal dimension. Let us consider the fractal to be covered by a 2D mesh of square cells of side r, which is varied. The number of boxes, N, occupied by the

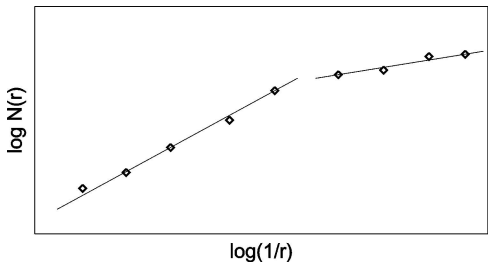

Figure 1. A slope of $\log(N)$ versus $\log(1/r)$ defines the fractal dimension, D_{f}. For natural fractals (i.e., for multifractals), the slope can change for different scale ranges.

fractal is proportional to the scale length, r, in a fractional power, D_{f}: $N(r) \sim r^{D_{\mathrm{f}}}$, which is called a fractal dimension. The fractal dimension can be approximated as a slope of $N(r)$ versus the inverse scale, $1/r$, in a double-logarithmic plot (Figure 1). Linearity of $\log(N(r))$ versus $\log(1/r)$ is called self-similarity. Computer-generated fractals are self-similar over an infinite range of scales. Such structures can be represented by one scalar parameter, D_{f}, and they are usually called monofractals.

However, in the case of natural fractals, self-similarity does not hold in the strict sense but does hold statistically over a finite range of scales. As soon as we deal with natural fractals, we immediately find that the slope of $\log(N)$ versus $\log(1/r)$ can change for different scale ranges (Figure 1). The cause of this may be just the nature of fractals and unavoidable influence of the process of data acquisition and processing. However, the latter is out of the scope of this paper (see, e.g., Lawrence, Cadavid, and Ruzmaikin, 1996; for more details on the estimation of the fractal dimension from digitized images of solar magnetic fields). Now, the entire range of scales can be divided into an infinite number of subsets, and for each subset its own self-similarity law holds with its own fractal dimension. Thus, a natural fractal may be treated as a multifractal, i.e. a superposition of an infinite number of monofractals. Local (in the sense of scale) character of self-similarity for natural fractals is one of the reasons to make a step from monofractals to multifractals.

Another reason is our intention to take into account the distribution of density in a fractal. In the case of solar magnetic fields, when we define a magnetic area as a binary mask (Figure 2) equal to unity on the set of all pixels where the absolute value of the magnetic field exceeds a given threshold (for example, 50 G, Figure 2, upper left frame), and to zero elsewhere, we obtain a fractal. By using, for example, the box-counting method, or some other methods (Takayasu, 1989), we can calculate the fractal dimension of the binary mask, which characterizes the complexity of its boundary. However, the fractal dimension can tell us nothing about the distribution of the magnetic field density *inside* the mask. It is well known that the density distribution may not be homogeneous. Moreover, the distribution of density determines the complexity of the magnetic structure and, therefore, the underlying physics. Thus, we have to incorporate the information on density. This

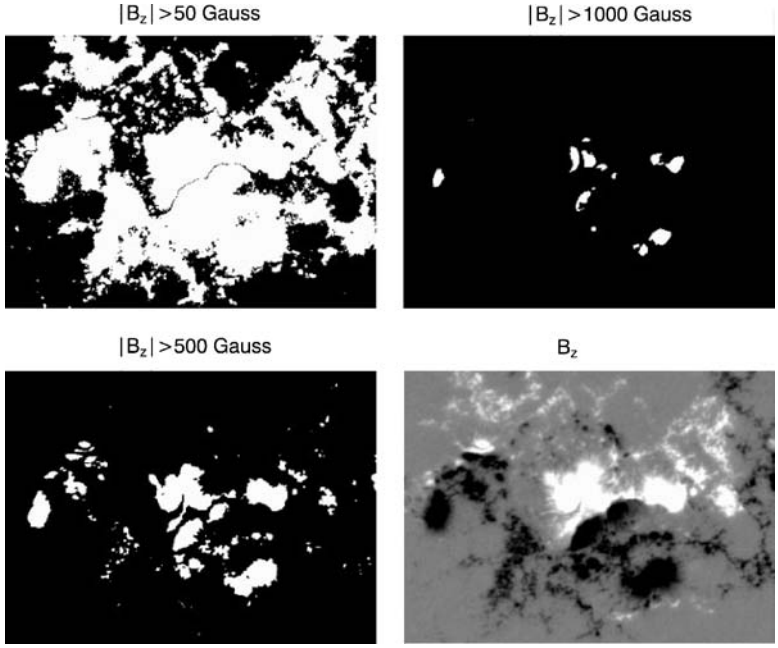

Figure 2. An hierarchy of binary masks of a solar magnetic structure (*lower right frame*). Each binary mask (*left frames* and *upper right frame*) is equal to unity on the set of all pixels where the absolute value of the magnetic field exceeds a given threshold (*noted above the frames*) and zero elsewhere. Superposition of infinite number of such masks/monofractals results in the observed magnetic structure, which is a multifractal (see the text).

can be done by introducing an hierarchy of masks defined by increasing threshold. The idea is illustrated in Figure 2: by specifying progressively higher thresholds, say, 500 G (lower left frame), 1000 G (upper right frame), we obtain new fractals and their parameters may vary. By incorporating these new monofractals, we can obtain addition information on the distribution of more and more dense patterns of the magnetic structure. The superposition of the infinite number of the monofractals results in a multifractal: a real distribution of the solar magnetic field (see lower right frame in Figure 2. Please, note that for simplicity sake, the sign of $B_{\|}$ on the masks was disregarded.) For a multifractal, a continuous spectrum of fractal parameters – a multifractal spectrum – is needed to characterize the structure. The broader the multifractal spectrum, the more complex the structure with a higher degree of multifractality it represents.

One more reason to incorporate multifractality is the existence of a highly intermittent character of structures arising in the evolution of the dynamic systems, where dissipative processes may not be neglected (such processes produce a majority of natural fractals). Intermittency implies a tendency of a certain quantity to concentrate into small-scale features of high intensity surrounded by extended areas of much lower fluctuations (Monin and Yaglom, 1975). Intermittency manifests

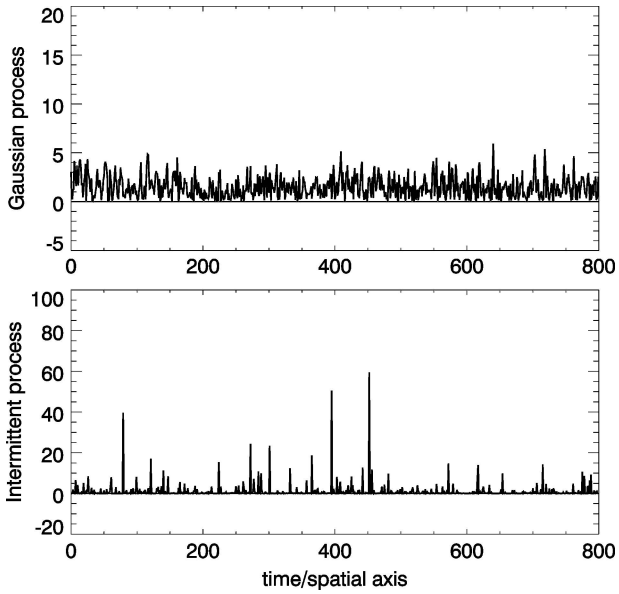

Figure 3. Illustration of phenomenological difference between a Gaussian process (*upper frame*), which is a non-intermittent and monofractal process of extremely rare large fluctuations, and an intermittent process (*lower frame*), which is a multifractal due to the contribution of large fluctuations (which are not so rare now) into the statistical moments. The horizontal axis may represent a time or a spatial coordinate.

itself via the burst-like behavior in temporal and spatial domains. Figure 3 demonstrates the phenomenological difference between a Gaussian process (which is non-intermittent) and an intermittent process. Large fluctuations in the intermittent process are not so rare as in the Gaussian process, and they contribute significantly into the statistical moments which leads to multifractality (see Frisch, 1995, for more details). Thus, by analyzing multifractality of a structure, we will also explore its intermittency. Generally, intermittency and multifractality are two different terms for the same phenomenon. Historically, the former term is usually applied to time series analysis, whereas the later one is used for spatial objects (Takayasu, 1989; Frisch, 1995). It is worthwhile to note that when a field is intermittent, the structure of its energy dissipation can not be homogeneous, but is intermittent, too (Monin and Yaglom, 1975; Frisch, 1995). Thus, by exploring intermittency of the magnetic field, one may also obtain valuable information on the behavior of the magnetic energy dissipation (Lawrence, Cadavid, and Ruzmaikin, 1995; Abramenko, 2003; Vlahos and Georgoulis, 2004).

There are several techniques to evaluate the degree of multifractality. In particular, for solar line-of-sight magnetograms, the box-counting method based on changing of the coarse-graining level was used by Lawrence, Ruzmaikin, and Cadavid (1993) and by Cadavid *et al.* (1994) to calculate the spectrum of fractal

dimensions. Other methods are based on the fractal measure relations, calculations of correlation and distribution functions (Takayasu, 1989), or structure functions (Frisch, 1995). Here I will show how structure functions can be used to evaluate the degree of multifractality in order to obtain benefits in solar image processing and learn more about solar magnetic fields.

2. Scaling of Structure Functions

Structure functions, defined as statistical moments of the increment of a field, are very useful non-traditional tools to study multifractality and intermittency (Stolovitzky and Sreenivasan, 1993; Frisch, 1995; Consolini *et al.*, 1999; Abramenko *et al.*, 2002).

In our case, the analyzed field is the line-of-sight component of the photospheric magnetic field, $B_\parallel$, so a structure function can be defined as follows:

$$S_q(r) = \langle |B_\parallel(\mathbf{x} + \mathbf{r}) - B_\parallel(\mathbf{x})|^q \rangle, \tag{1}$$

where $\mathbf{x}$ is each point on a magnetogram, $\mathbf{r}$ the separation vector, and q the order of a statistical moment, which takes on real values. Angular brackets denote averaging over the magnetogram. Within some range of scales, when plotted in a double logarithmic plot, structure functions are linear. The slope, $\zeta(q)$, is then a function of the statistical moment, q. Figure 4 shows an example of the structure functions (upper left frame) and the corresponding $\zeta(q)$ function (upper right frame) calculated from one line-of-sight magnetogram of an active region.

When the field under study is a monofractal, then $\zeta(q)$ is a straight line. However, for multifractals, $\zeta(q)$ appears to be a concave function and then its derivative $h(q) = \mathrm{d}\zeta(q)/\mathrm{d}q$ is not a constant value, so that h varies within some range Δh. For each value of h there is a fractal with an h-dependent dimension, $D(h)$. (According to Frisch (1995), h and $D(h)$ are related by the Legendre transform, however, calculation of $D(h)$ is beyond the scope of this paper.) Thus, multifractality of the field is manifested via concavity of $\zeta(q)$ function. I will accept the value $\Delta h \equiv h_{\max} - h_{\min}$ (Figure 4, lower right frame) as an estimation of the degree of multifractality of the field. Indeed the larger Δh, the broader the set of monofractals which together form the resulting multifractal.

The weakest point in the above technique is determination of the scale range, Δr, where the slope $\zeta(q)$ is to be calculated. To visualize the range of multifractality, Δr, I suggest using the flatness function. Generally, the ratio of the fourth statistical moment to the square of the second statistical moment determines the flatness function. However, when analyzing multifractality, Frisch (1995) suggested using higher statistical moments to calculate the (hyper-)flatness, namely, the ratio of the sixth moment to the cube of the second:

$$F(r) = S_6(r)/(S_2(r))^3. \tag{2}$$

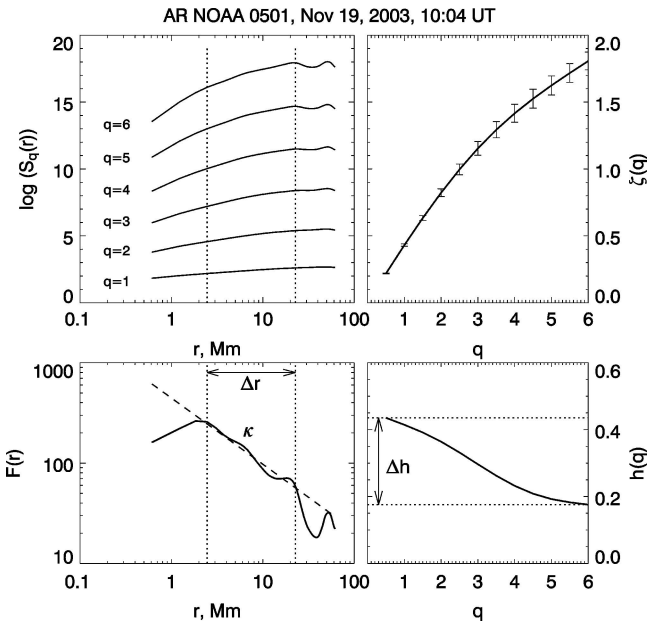

Figure 4. Structure functions $S_q(r)$ (*upper left*) calculated from a magnetogram of active region NOAA 0501 by Equation (1). *Lower left*: flatness function $F(r)$ calculated from the structure functions by Equation (2). *Vertical dotted lines* mark the interval of multifractality, Δr, where flatness grows as power law when r decreases. The interval Δr is also marked in upper left frame. κ is the power index of $F(r)$ determined within Δr. The slope of $S_q(r)$, defined for each q within Δr, is the $\zeta(q)$ function (*upper right*), a concave for a multifractal and straight line for a monofractal. *Lower right*: function $h(q)$ is a derivative of $\zeta(q)$. The interval between the maximum and minimum values of $h(q)$ is defined as a degree of multifractality, Δh.

Equation (2) was used to calculate $F(r)$ and, for simplicity, I will refer to $F(r)$ as the flatness function. For monofractal structures, the flatness does not depend on the scale, r. On the contrary, for a multifractal structure, the flatness grows as a power-law, when the scale r decreases (Frisch, 1995). Usually, when studying natural fractals, the range Δr of the flatness's growth is bounded (see lower left frame in Figure 4). Possible causes of the boundness of the interval of multifractality were not comprehensively studied yet (Frisch, 1995).

The slope, κ, of flatness function, determined within Δr, (Figure 4) seems to be related to the degree of multifractality: the steeper the function $F(r)$, the higher the degree of multifractality.

3. Diagnostics of Image Defects

As it was discussed above, a random field with Gaussian distribution of density is a monofractal. The method was applied first to such a Gaussian field with a zero

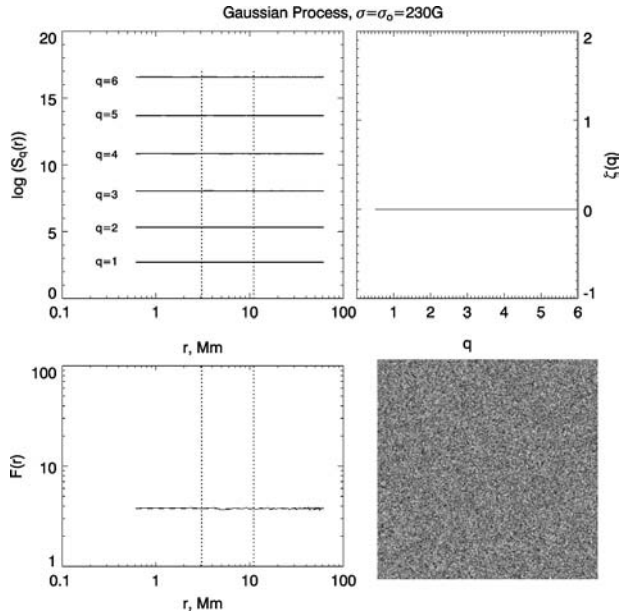

Figure 5. Structure functions $S_q(r)$, flatness function $F(r)$ and $\zeta(q)$ function calculated from an artificial Gaussian field (*lower right*). Other notations are the same as in Figure 4.

mean value and the standard deviation $\sigma_0 = 230$ G, that was chosen to be the same as those obtained from high-resolution magnetograms of active regions. The result is presented in Figure 5, and it shows that for a monofractal structure, the code produces the correct result with $\Delta h = 0$ and $F(r) = \text{const}$.

Then the standard deviation was increased three-fold, a 5×5 point box-car running averaging was applied and the calculations were repeated again. In this case, a constant flatness and vanishing degree of multifractality were also obtained (figures are not shown). This experiment shows that results of the study of the multifractality, obtained by the proposed method, seem to be not contaminated by the changes in the noise level and seeing, which, plausibly, produce Gaussian structures.

However, when an artificial "hot" pixel was added (a pixel with extremely high artificial density) in the magnetogram, the flatness begins to curve up at small scales (Figure 6). The reason for that is that the presence of extremely large fluctuations implies intermittency, in other words, multifractal organization of a field (see Figure 3). This property of flatness was used to automatically select and discard magnetograms with "hot" pixels present in them.

Next, a large-scale distortion in a magnetogram was modeled in order to mimic an uncorrected flat field: to the smoothed Gaussian magnetogram a gradual function $A \cos(2\pi x L)$ was added. Here x is the horizontal coordinate on the map, L is the total size in the x direction and A is a free parameter (see Figure 7, lower right frame). For this "uncorrected" magnetogram, the flatness function, $F(r)$, curves

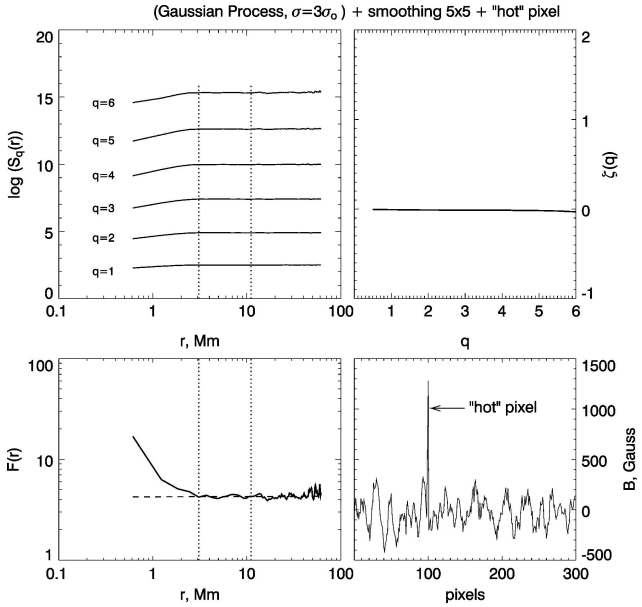

Figure 6. Structure functions $S_q(r)$, flatness function $F(r)$ and $\zeta(q)$ function, calculated from a smoothed Gaussian field with artificially added extremely high fluctuation in one of pixels ("hot" pixel). *Lower right*: a scan across the "hot" pixel. Other notations are the same as in Figure 4.

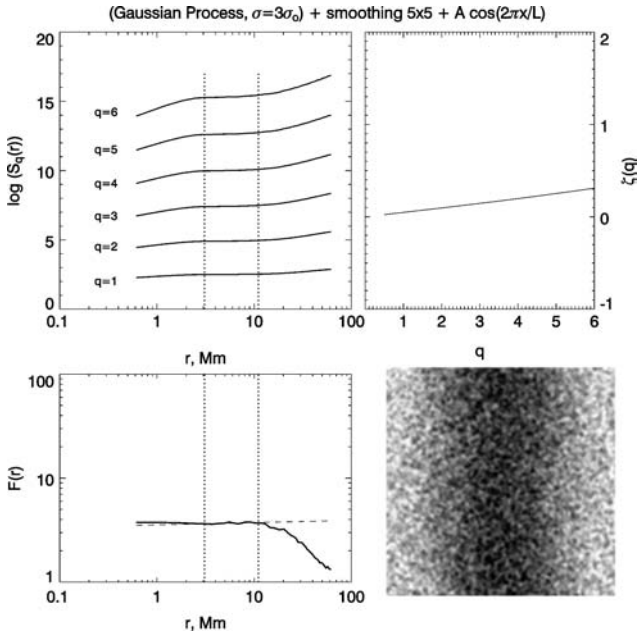

Figure 7. Structure functions $S_q(r)$, flatness function $F(r)$ and $\zeta(q)$ function, calculated from an artificial magnetogram (*lower right*) which is a smoothed Gaussian field with artificially added function $A\cos(2\pi x/L)$. Other notations are the same as in Figure 4.

down at large scales (see Figure 7, lower left frame). Therefore, this property of flatness may be used for diagnostics of the quality of the flat field correction.

An experiment in analyzing a sequence of magnetograms of high time cadence (say, 1 min) for a given active region showed that functions $S_q(r)$, $F(r)$, $\zeta(q)$ and $h(q)$ vary very gradually from one magnetogram to another. Any defect in a magnetogram caused by the instrument (e.g., "hot" pixels, vignetting, flat field non-uniformity, etc.) is immediately reflected via sharp changes in the shape of the flatness function and, to a lesser degree, in the shape of the rest of the functions. This property of $F(r)$ was used to select and automatically discard bad quality magnetograms.

4. Multifractality of the Magnetic Field in Active Regions

As for any other multiscale method, data of the highest available resolution and sensitivity are desirable to use for the proposed code in order to trace the finest real features. Moreover, different active regions observed with *the same* instrument should be analyzed at the first stage of the code testing. Thus, in the present study the code was applied to magnetograms of different solar active regions obtained in the high resolution (HR) mode by the Michelson Doppler Imager (MDI) instrument (Scherrer *et al.*, 1995) on board the Solar and Heliospheric Observatory (SOHO). The pixel size of the magnetograms is 0.58×0.58 arcsec. The HR mode of SOHO/MDI can register active regions located only within the central parts of the solar disk.

The next stage of the code testing will be the comparison of results obtained with different instruments, which is a subject for further publications. Application of the first version of our code (without the flatness function) to the ground-based data can be found in Abramenko *et al.* (2002, 2003).

The result of the calculations for two active regions, NOAA 9077 and 0061, are presented in Figures 8 and 9, respectively. One can see that the scaling behavior of the structure functions is rather different in these active regions. For the first one, NOAA AR 9077, there exists a well-defined range of scales, $\Delta r = (4\text{–}23)$ Mm where flatness $F(r)$ grows with the power index $\kappa = -1.17$ as r decreases. The function $\zeta(q)$ is concave and the corresponding $\Delta h \approx 0.5$. The result implies a multifractal structure of the magnetic field in this active region.

On the contrary, in NOAA AR 0061 (Figure 9) the flatness function oscillates around a horizontal line, which implies a monofractal character of the magnetic field. The function $\zeta(q)$ is almost a straight line that produces a vanishing value of $\Delta h \approx 0.05$.

Time profiles of Δh for the two active regions are compared in Figure 10. Two 6-h data sets allowed us to conclude that NOAA AR 0061 persistently displays a lower degree of multifractality, as well as a lower level of X-ray emission than NOAA AR 9077 does. Note that NOAA AR 0061 was the only strong feature on the

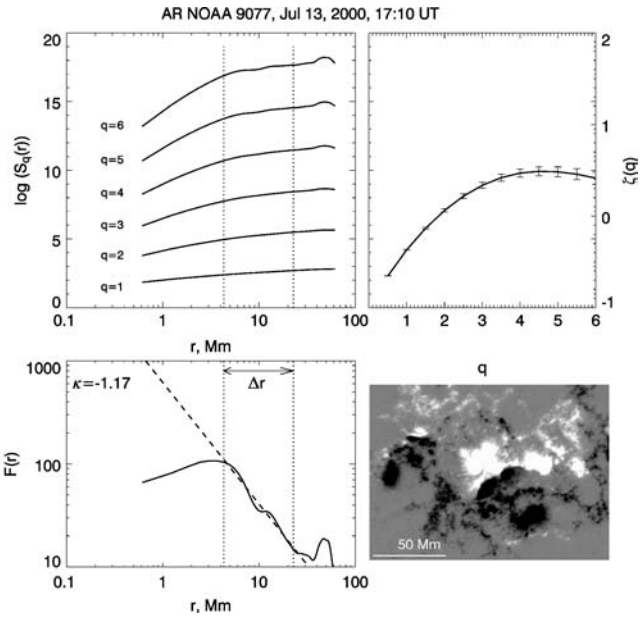

Figure 8. Structure functions $S_q(r)$, flatness function $F(r)$ and $\zeta(q)$ function from one magnetogram of active region NOAA 9077 (*lower right*). κ is a power-law index of $F(r)$ calculated inside Δr. The degree of multifractality for this magnetogram $\Delta h = 0.48$. Other notations are the same as in Figure 4.

solar disk, thus the GOES flux time profile can be associated with the activity in this region. As to NOAA AR 9077, Big Bear Solar Observatory Ca II K images show that the gradual M1.2 flare (marked by an arrow in Figure 10) was launched in a mature active region 9077, whereas other GOES-flux peaks during the time period under study seem to be associated with another, rather moderate, active regions on the periphery of the solar disk.

It is appropriate to mention here that the two active regions displayed very different flare productivity. Active region 9077 was very flare productive: during the passage across the solar disk, it launched 37 flares of X-ray class higher than C3, including 13 M-class flares and 3 X-class flares. One of them was the famous "Bastille Day" flare of X5.7 class launched on July 14, 2000 at 10:04 UT. Active region 0061, on the contrary, produced only six flares of X-ray class lower than C3 during its passage across the solar disk.

It also is worthwhile to note here that the third active region analyzed in the present study, NOAA AR 0501, showed both intermediate (between AR 0061 and AR 9077) flaring productivity, and intermediate multifractality (compare Figures 4, 8 and 9). Our previous study of multifractality for eight active regions (Abramenko *et al.*, 2002) showed a similar tendency: active regions of low flaring activity tend to possess a lower degree of multifractality than active regions of high flaring activity do (see Figures 4 and 5 in Abramenko *et al.*, 2002). Both results seem to suggest

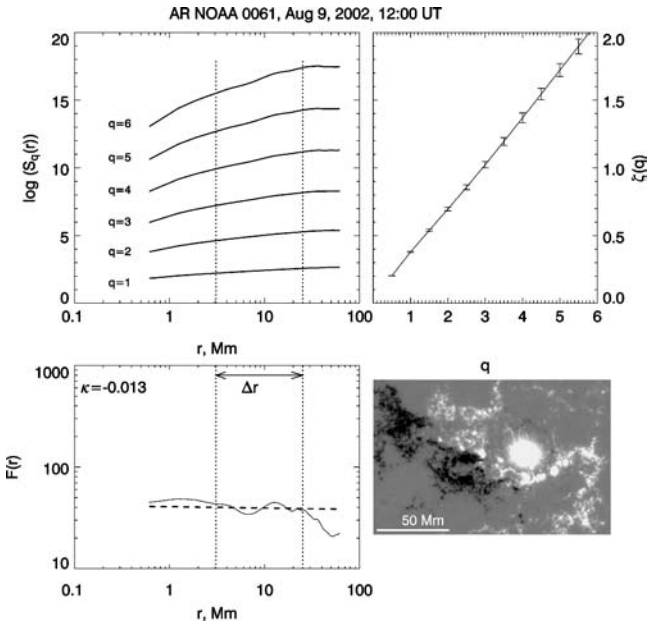

Figure 9. Structure functions $S_q(r)$, flatness function $F(r)$ and $\zeta(q)$ function from one magnetogram of active region NOAA 0061 (*lower right*). Other notations are the same as in Figure 4. Note that for this active region, the function $\zeta(q)$ is a nearly straight line with the vanishing degree of multifractality $\Delta h = 0.058$.

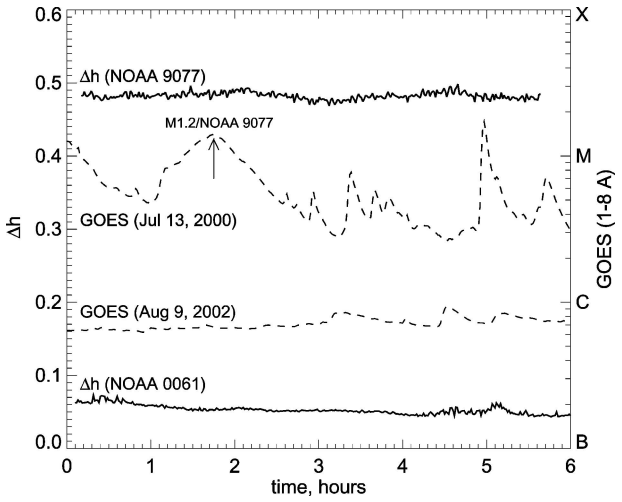

Figure 10. Time variations of the measure of multifractality, Δh (*left axis*), and GOES soft X-ray flux (*right axis, dashed lines*) plotted for 6-h time intervals for the two active regions. Data for NOAA AR 9077 (*black lines*) were obtained between 17:00 and 23:00 UT on July 13, 2000. The *arrow* marks the M1.2 flare that occurred in NOAA AR 9077, whereas other peaks of the GOES flux are associated with other active regions on the solar disk. Data for NOAA AR 0061 (*gray lines*) refer to an interval between 11:00 and 17:00 UT on August 9, 2002.

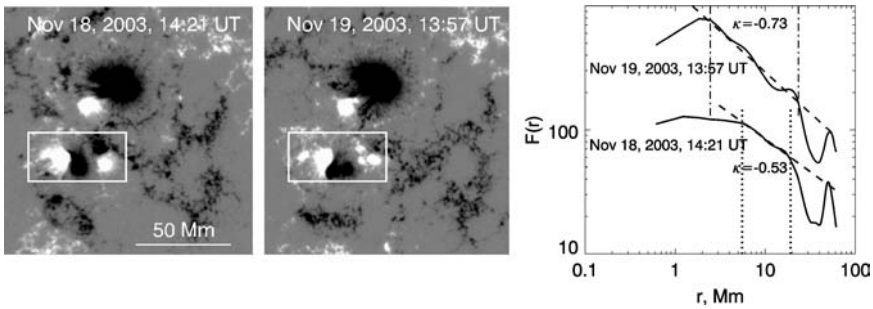

Figure 11. Two magnetograms of NOAA AR 0501 obtained on November 18, 2003 at 14:21 UT and on November 19, 2003 at 13:57 UT. An area where the fragmentation of magnetic elements is the most noticeable, is marked by white boxes. *Right*: flatness functions $F(r)$ for two magnetograms. Gray curve, corresponding to the later magnetogram, is shifted up into a "well-readable" position. The range of multifractality, Δr, for the earlier magnetogram is indicated by the *dotted lines*, whereas the more broad Δr for the later magnetogram is marked by *dash-dotted lines*. κ is the power index of $F(r)$ calculated as a linear best fit (*dashed lines*) inside the corresponding intervals Δr.

that the multifractality of the photospheric magnetic field may be related to the flare productivity of an active region. Of course, a broad statistical study is needed to verify this suggestion.

Day-to-day changes in the flatness function for active region 0501 are presented in Figure 11. During the 24-h time interval between magnetograms the flatness function became steeper ($\kappa = -0.53$ for the earlier data and -0.73 for the later data) and the range of multifractality, Δr, extended considerably, from $\Delta r = (5.5\text{–}19)$ Mm to $\Delta r = (2.5\text{–}22)$ Mm. The degree of multifractality also increased from 0.18 to 0.29. Comparison of the magnetograms, presented in the left part of Figure 11, suggests a reinforcement of a fragmentation of magnetic elements during the discussed time period. Indeed, the magnetic field in the November 19, 2003 magnetogram became more fragmented, especially inside the white box, where some large magnetic structures disappeared while many small-scale features appeared in their places. Reinforcement of fragmentation seems to be the cause of the extension of the range of multifractality. In this case the increase of multifractality seems to be plausible, because the intensification of the fragmentation process may lead to a highly intermittent, multifractal structure of solar magnetic field (Abramenko and Longcope, 2005).

5. Summary and Discussion

This paper presents further elaboration of the approach proposed by Abramenko *et al.* (2002) to analyze properties of multifractality of solar magnetograms. The approach is based on calculations of the structure functions $S_q(r)$ that are defined as the statistical moments of the increment of a field under study. Scaling characteristics of the structure functions allow to estimate the degree of multifractality, Δh, of

the field. In the present study a new scaling characteristic of the structure functions, namely, the flatness function $F(r)$, is proposed for the analysis of multifractality. It is shown that the scale interval of multifractality, Δr, can be visualized from the flatness function. Correct determination of Δr is important for estimation of the degree of multifractality and may also have independent physical applications in future. Determination of multifractality with the code proposed seems not to be dependent on parameters of the Gaussian background of the digitized image of the magnetic field.

Application of the code to magnetograms of solar active regions showed that the structure functions and their scaling characteristics differ for the active regions studied. For a given active region, the shape of the functions may remain unchanged during several hours. However, the structure functions can noticeably change during a day. Thus, in NOAA AR 0501, the extension of the range of multifractality from $\Delta r = (5.5–19)$ Mm to $\Delta r = (2.5–22)$ Mm and the increase of the degree of multifractality from $\Delta h = 0.18$ to $\Delta h = 0.29$ was accompanied by a noticeable fragmentation of magnetic flux concentrations during a 24-h period. This seems to be in a good agreement with the result reported by Abramenko and Longcope (2005), which suggests that one possible cause of the increase of multifractality in the photospheric magnetic field is the process of fragmentation of magnetic elements.

There are reasons to assume that multifractality has different character in flaring and flare-quiet active regions. Namely, flare-quiet active regions tend to display a lower degree of multifractality than flaring active regions do. Thus, in the present study, flare-quiet active region NOAA AR 0061 during 6-h period of observations showed a very low level of multifractality $\Delta h = 0.060 \pm 0.007$, while in the flaring active region 9077 the degree of multifractality, determined during a 6-h interval, was almost 10 times stronger, $\Delta h = 0.50 \pm 0.01$.

The amplification of multifractality means, on one hand, appearance of large fluctuations and, on the other hand, extension of areas of low fluctuations (see Figure 3). For the magnetic field, it is equivalent to emergence (or intensification) of small-scale flux tubes carrying very strong flux. However, emergence of large-scale (nearly homogeneous) magnetic structures may also contribute into the increase of multifractality. This increase may be an indication that a magnetic structure is driven to a critical state (Charbonneau *et al.*, 2001; Vlahos and Georgoulis, 2004) by gaining tangential discontinuities (Parker, 1987, 1996) of various length scales. In this case, the above suggestion about the possible relation between the character of multifractality and level of flare productivity seems to be reasonable and deserves further investigation.

The concept of multifractality of solar structures and, especially, solar magnetic fields can be used to gain deeper insight into the processes occurring in non-linear dissipative dynamical systems such as magnetized plasma in the solar atmosphere.

A byproduct of the proposed method is the possibility to automatically control images quality: the flatness function varies very gradually with time, so that any

abrupt changes in the shape of flatness function are a signal of a possible degradation of the image.

Acknowledgements

The author thanks Peter Gallagher, James McAteer, David Rust and Vasyl Yurchyshyn for helpful discussion of these results. I am also grateful to the anonymous referee, whose comments helped to improve this paper. SOHO is a project of international cooperation between ESA and NASA. This work was supported by NSF-ATM 0076602, 0205157, 0233931 and NASA NAG5-12782 grants.

References

Abramenko, V. I.: 2003, *Astron. Rep.* **47**, 151.
Abramenko, V. I. and Longcope, D. W.: 2005, *Astrophys. J.* **619**, 1160.
Abramenko, V. I., Yurchyshyn, V. B., Wang, H., Spirock, T. J., and Goode, P. R.: 2002, *Astrophys. J.* **577**, 487.
Abramenko, V. I., Yurchyshyn, V. B., Wang, H., Spirock, T. J., and Goode, P. R.: 2003, *Astrophys. J.* **597**, 1135.
Balke, A. C., Schrijver, C. J., Zwaan, C., and Tarbell, T. D.: 1993, *Solar Phys.* **143**, 215.
Cadavid, A. C., Lawrence, J. K., Ruzmaikin, A. A., and Kayleng-Knight, A.: 1994, *Astrophys. J.* **429**, 391.
Charbonneau, P., McIntosh, S. W., Liu, H. L., and Bogdan, T. J.: 2001, *Solar Phys.* **203**, 321.
Consolini, G., Berrilli, E., Pietropaolo, E., Bruno, R., Carbone, V., Bavassano, B., and Ceppatelli, G.: 1999, in *Magnetic Fields and Solar Processes*, ESA SP-448, Paris, ESA, p. 209.
Feder, J.: 1988, *Fractals*, Plenum Press, New York and London.
Frisch, U.: 1995, *Turbulence, The Legacy of A.N. Kolmogorov*, Cambridge University Press, Cambridge.
Lawrence, J. K., Ruzmaikin, A. A., and Cadavid, A. C.: 1993, *Astrophys. J.* **417**, 805.
Lawrence, J. K., Cadavid, A. C., and Ruzmaikin, A. A.: 1995, *Phys. Rev. E* **51**, 316.
Lawrence, J. K., Cadavid, A. C., and Ruzmaikin, A. A.: 1996, *Astrophys. J.* **465**, 425.
Mandelbrot, B.: 1977, *Fractals: Form, Chance and Dimension*, Freeman and Co., San Francisco.
McAteer, R. T. J., Gallagher, P. T., and Ireland, J.: *Astrophys. J.*, in press.
Meunier, N.: 1999, *Astrophys. J.* **515**, 801.
Monin, A. S. and Yaglom, A. M.: 1975, in J. Lumley (ed.), *Statistical Fluid Mechanics*, Vol. 2, MIT Press, Cambridge, MA.
Parker, E. N.: 1987, *Solar Phys.* **111**, 297.
Parker, E. N.: 1996, *Solar Phys.* **169**, 327.
Scherrer, P. H., Bogart, R. S., Bush, R. I., Hoeksema, J. T., Kosovichev, A. G., Schou, J., Rosenberg, W., Springer, L., Tarbell, T. D., Title, A., Wolfson, C. J., Zayer, I., and the MDI Engineering Team: 1995, *Solar Phys.* **162**, 129.
Stolovitzky, G. and Sreenivasan, K. P.: 1993, *Phys. Rev. E* **48**, R33.
Takayasu, H.: 1989, *Fractals in the Physical Sciences*, Manchester University Press, Manchester and New York.
Vlahos, L. and Georgoulis, M. K.: 2004, *Astrophys. J.* **603**, L61.